

Sticky Normal/Superconductor Interface

Soo-Young Lee,¹ Arseni Goussev,^{1,2} Orestis Georgiou,¹ Goran Gligorić,³ and Achilleas Lazarides^{1,*}

¹Max Planck Institute for the Physics of Complex Systems, Nöthnitzer Str. 38, D01187 Dresden, Germany

²Department of Mathematics and Information Sciences, Northumbria University, Newcastle Upon Tyne, NE1 8ST, United Kingdom

³Vinca Institute of Nuclear Sciences, University of Belgrade, P. O. Box 522, 11001 Belgrade, Serbia
(Dated: December 27, 2012)

We study the quantum Goos-Hänchen (GH) effect for wave-packet dynamics at a normal/superconductor (NS) interface. We find that the effect is amplified by a factor (E_F/Δ) , with E_F the Fermi energy and Δ the gap. Interestingly, the GH effect appears only as a time delay δt without any lateral shift, and the corresponding delay length is about $(E_F/\Delta)\lambda_F$, with λ_F the Fermi wavelength. This makes the NS interface “sticky” when $\Delta \ll E_F$, since typically GH effects are of wavelength order. This “sticky” behavior can be further enhanced by a resonance mode in NSNS interface. Finally, for a large Δ , the resonance-mode effect makes a transition from Andreev to the specular electron reflection as the width of the sandwiched superconductor is reduced.

PACS numbers: 03.65.Vf, 74.45.+c, 73.40.-c

Interference is an important phenomenon in both quantum and wave mechanics, and is often responsible for intriguing effects not understandable from a classical mechanics and ray dynamics. The Goos-Hänchen (GH) effect [1], first predicted by Newton, is one example: When an optical beam is totally reflected at a dielectric interface, a lateral shift along the interface is induced. The GH shift has been studied in various quantum and wave systems, amongst which graphene [2, 3], optical beams [4], dielectric microcavities [5–7] and neutrons [8].

The GH shift in optics can be understood by the dependence of the phase loss occurring at total internal reflection [9] on the angle of incidence. An analogous shift is observed in the quantum mechanical step potential problem: In the one dimensional case, if the energy E of an incident particle is less than the potential height V , the particle is totally reflected with reflection coefficient is $R = e^{i\varphi}$ (with real φ). The phase φ increases monotonically from $-\pi$ to zero as the energy E varies from zero to V . If we consider an incident Gaussian wave packet with velocity $v_0 = \hbar k_0/m$,

$$\psi_I(x, t) = \int dk g(k) e^{ikx} e^{-iEt/\hbar}, \quad (1)$$

where $g(k) = e^{-(k-k_0)^2/\sigma^2}$, σ is the width of the Gaussian window, and $E = (\hbar k)^2/2m$, the wave packet reflected off the step potential at $x = 0$ becomes

$$\psi_R(x, t) = \int dk g(k) R e^{-ikx} e^{-iEt/\hbar}. \quad (2)$$

The stationary phase approximation gives a time-delayed motion of the centre of the wave packet, $x = -v_0(t - \delta t)$,

with the time delay given by

$$\delta t = \hbar \frac{d\varphi}{dE}. \quad (3)$$

As a result, the delay length $l_D \equiv v_0 \delta t$ is $l_D \sim \lambda_0$ with $\lambda_0 = 2\pi/k_0$ the central wavelength of the wave packet. For a wave packet propagating in two dimensions with y -direction velocity v_{0y} , the time delay results in a lateral shift of $l_{GH} = v_{0y} \delta t$, analogously to the optical GH shift. Note that the GH shift here is of the order of a wavelength. This δt is similar to the Wigner delay time in scattering problems [10]. The phase change φ is also related to the non-integer Maslov index for the quantization condition [11].

On the other hand, the behavior of an electron or a hole at normal/superconductor (NS) interface has been studied extensively. For a small superconducting pairing gap Δ ($\sim 10^{-4} E_F$) an incident electron from the normal side is retro-reflected as a hole when the excitation energy is less than the pair gap Δ of the superconductor; this is called Andreev reflection [12], and has been studied in systems as diverse as graphene [13] and bosonic condensates [14]. It has been directly experimentally observed [15]. In addition, the advance of laser cooling techniques for atoms allows experimental realization of a similar interface with a large Δ comparable to the Fermi energy E_F , where specular reflection of particles (in addition to Andreev reflection of holes) occurs with appreciable amplitude [16–18]. In spite of much attention to the electronic properties at the NS interface, the phase change under reflection has not been explored so far. It is therefore desirable to understand the influence of the phase change on reflection off the NS interface and the associated GH effect.

In this Letter, we study reflection off NS and NSNS interfaces and find that the GH effect is amplified by a factor (E_F/Δ) compared to that of other interfaces. This is because at the NS interface the incident electron can be reflected within the energy scale of Δ , while the wave-

*Electronic address: acl@pks.mpg.de

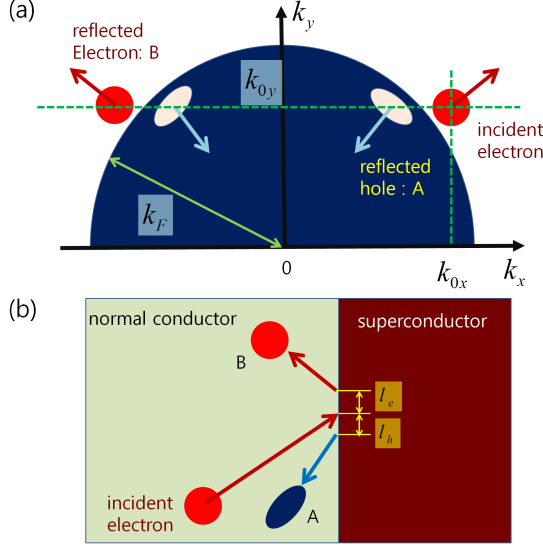


FIG. 1: (color online) (a) Schematic diagram for electron and hole excitations near the Fermi surface in (k_x, k_y) plane. The arrows indicate the direction of group velocity of the corresponding wave packets. (b) The real-space illustration of the excitations in (a). An incident electron can be bounced into a hole (A) and an electron (B). l_e and l_h are GH shifts expected from a naive extension of the step-potential case, but they turn out to be zero in this NS interface (see Fig. 2 and 4).

length is determined by the whole energy scale of $\sim E_F$. Moreover, the GH effect appears as a time delay without the lateral shift which has been the hallmark of the GH effect in other interfaces. The corresponding delay length is then given by $l_D \sim (E_F/\Delta)\lambda_F$, where λ_F is the Fermi wavelength, implying that the NS interface is very “sticky” in comparison to typical wavelength-order delay lengths in optical and condensed-matter interfaces. We also show that the time delay can be increased by a resonance mode in NSNS interface. Finally, for a large gap Δ ($\sim E_F$) the resonant reflection exhibits a transition from Andreev retroreflection to specular electron reflection as reducing the width of sandwiched superconductor.

In what follows, we describe our theoretical setup, then begin our study with the $\Delta/E_F \ll 1$ for both NS and NSNS interfaces. We then turn to the general Δ/E_F case, for which we discuss the crossover between Andreev and specular reflection before drawing our conclusions.

In a superconductor, electrons and holes are coupled to each other with a coupling strength given by the pair gap Δ ; this situation is described using the Bogoliubov-de Gennes (BdG) equations for a two-component wave function Ψ [19, 20]:

$$\begin{pmatrix} H & \Delta \\ \Delta & -H \end{pmatrix} \Psi = \varepsilon \Psi, \quad (4)$$

with

$$H = -\frac{\hbar^2}{2m} \nabla^2 - \mu, \quad \Psi = \begin{pmatrix} u \\ v \end{pmatrix} \quad (5)$$

where ε is the energy measured from the chemical potential μ ($\mu = E_F$ in our case) while u and v are the electron and hole wave functions, respectively. The pair gap Δ is zero in a normal conductor, i.e., the electron and hole are independent of each other. We also assume that Δ is a real number, that is, we consider an s -wave superconductor and a static situation.

We begin by focussing on the case of an incident electron with an energy ε ($< \Delta$) as schematically illustrated in Fig. 1. From the BdG equation, the two independent plane-wave solutions [12, 21] with the same y -dependence $e^{ik_y y}$ are

$$\Psi_e = \begin{pmatrix} 1 \\ \frac{\varepsilon - \Omega}{\Delta} \end{pmatrix} e^{i(k_e x + k_y y)}, \quad \Psi_h = \begin{pmatrix} \frac{\varepsilon - \Omega}{\Delta} \\ 1 \end{pmatrix} e^{i(k_h x + k_y y)}, \quad (6)$$

where $\Omega = \sqrt{\varepsilon^2 - \Delta^2}$ and

$$k_e = \sqrt{k_{Fx}^2 + \frac{2m}{\hbar^2} \Omega}, \quad k_h = \sqrt{k_{Fx}^2 - \frac{2m}{\hbar^2} \Omega}, \quad (7)$$

where $k_{Fx} = \sqrt{\frac{2m}{\hbar^2} E_F - k_y^2}$ and it becomes Fermi wavenumber k_F when $k_y = 0$. Note that in the normal conductor with zero Δ , the solutions become independent electron (u) and hole (v) wavefunctions since $(\varepsilon - \Omega)/\Delta = 0$ in Eq.(6), and their wavenumbers, k_e^N and k_h^N , are given by Eq.(7) with $\Omega = \varepsilon$.

We obtain the reflection coefficients for the reflected electron and hole plane waves by matching wavefunctions at the interface ($x = 0$). The wavefunction in the normal part is

$$\Psi_N = \begin{pmatrix} e^{ik_e^N x} + B e^{-ik_e^N x} \\ A e^{ik_h^N x} \end{pmatrix} e^{ik_y y}, \quad (8)$$

while the wave function in the superconductor is Ψ_S with decaying u and v for our case of $\varepsilon < \Delta$. From $\Psi_N(0) = \Psi_S(0)$ and $\Psi'_N(0) = \Psi'_S(0)$, we can obtain the reflection coefficients A (hole) and B (electron).

In order to study a dynamical situation, we now switch to an incident wave packet rather than a plane wave. The incident electron with an average wavevector $\vec{k}_0 = (k_{0x}, k_{0y})$ can be described as a Gaussian wave packet,

$$u_I(\vec{x}, t) = \int dk_x dk_y \mathcal{G}(\vec{k}) e^{i(k_x x + k_y y - \varepsilon t/\hbar)} \quad (9)$$

where $\mathcal{G}(\vec{k}) = e^{-|\vec{k} - \vec{k}_0|^2/\sigma^2}$ and $\varepsilon = (\hbar^2 |\vec{k}|^2/2m) - E_F$. Note that at $t = 0$ the wave packet hits the interface located at $x = 0$. The reflected hole is then represented by

$$v_R(\vec{x}, t) = \int dk_x dk_y \mathcal{G}(\vec{k}) A e^{i(k_h^N x + k_y y - \varepsilon t/\hbar)}, \quad (10)$$

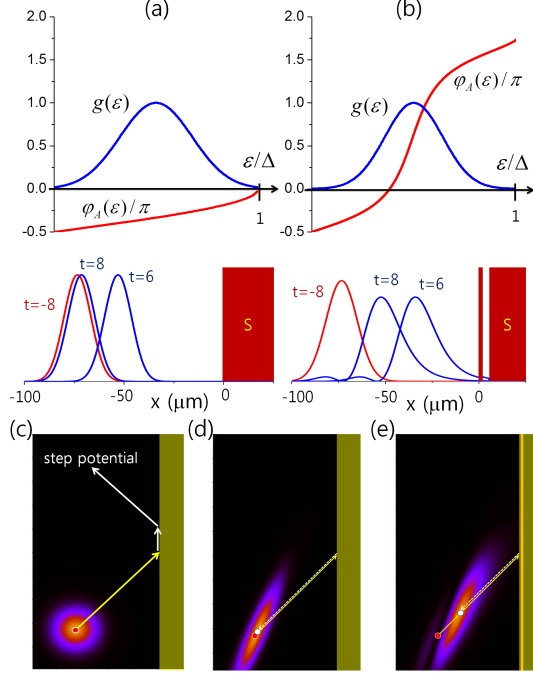


FIG. 2: (color online) Wave-packet dynamics when $\Delta = 10^{-4} E_F$. (a) The phase φ_A (red line) and the Gaussian window function $g(\varepsilon)$ (blue line) used. In the lower pannel, electron wave packets (red line) at $t = -8$ and reflected hole wave packets (blue lines) at $t = 6, 8$ are shown. (b) The same as (a) for the resonant reflection in the NSNS interface with $(d, L) = (1, 4)$. (c,d,e) Wave-packet dynamics with 45 degree incident angle. The scale of the normal conductor shown above is $(100 \times 200) \mu\text{m}^2$. (c) The incident-electron wave packet at $t = -10$. The yellow arrow denotes the incident path. The white arrows show schematically a typical GH shift of the step-potential case. (d) Andreev reflection. The reflected-hole wave packet at $t = 10$ is shown. (e) The same as (d) in the NSNS interface with $(d, L) = (0.8, 2.8)$. The delay length corresponds to the distance between initial (red dot) and final position (white dot). Here, the units of length and t is μm and $6.58 \times 10^{-12} \text{s}$, respectively. (see supplemental material for wave-packet animations)

and the wave packet for the reflected electron can be obtained by the replacements $A \rightarrow B$ and $k_h^N \rightarrow -k_x$ in the above equation (see Fig. 1 (a)). For the normal incidence case $k_{0y} = 0$, it is easy to get time delay from the stationary phase point: The peak position of the reflected hole is given by

$$x = \frac{v_{0x}}{dk_h^N/dk_x}(t - \delta t_x^A), \quad \delta t_x^A = \hbar \frac{d\varphi_A}{d\varepsilon}, \quad (11)$$

where φ_A is the phase of A . Similarly, for the reflected electron we find $\delta t_x^B = \hbar(d\varphi_B/d\varepsilon)$.

We now concentrate on the case of relevance to solid-state and liquid helium experiments [15], $\Delta \ll E_F$, specifically with $\Delta/E_F = 10^{-4}$ which is the typical value in solid-state superconductors. We set the Fermi energy as $E_F = 5.5 \text{ eV}$ throughout this Letter. This case corresponds to Andreev reflection [12], so that only the retro-

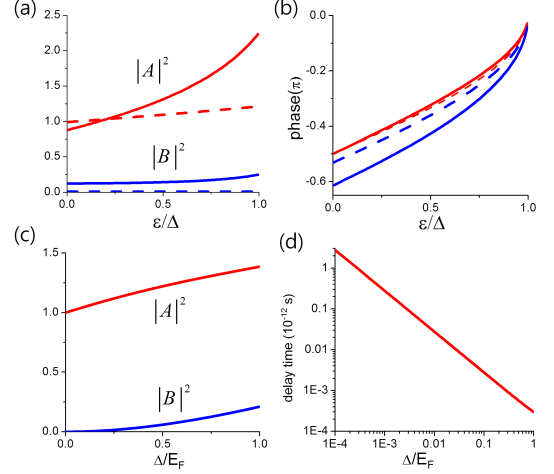


FIG. 3: (color online) (a) $|A|^2$ (red) and $|B|^2$ (blue) are shown as a function of ε , when $\Delta = 0.2 E_F$ (dashed line) and $\Delta = 0.8 E_F$ (solid line). (b) The corresponding phases, φ_A (red) and φ_B (blue). (c) Change of $|A|^2$ (red) and $|B|^2$ (blue) evaluated at $\varepsilon = 0.5\Delta$ with increasing Δ . (d) The corresponding delay time δt^A as a function of Δ .

reflected hole has appreciable amplitude ($|A| \simeq 1$ and $|B| \simeq 0$). The phase φ_A is drawn in Fig. 2 (a) and it is well approximated by $\varphi_A = \arccos(\varepsilon/\Delta)$ when $B = 0$. This phase variation enables us to calculate the delay time and length, defined by $l_D \equiv v_F \delta t_x^A$, v_F is the Fermi velocity. We emphasize that the delay length is amplified by a factor (E_F/Δ) , i.e.,

$$l_D \simeq \left(\frac{E_F}{\Delta} \right) \lambda_F, \quad (12)$$

which is a distinctive feature of the NS interface, noting that typical shifts in other interfaces are wavelength-order. Thus the NS interface can be characterized as “sticky” due to the long-time stay at the interface.

Since the delay time is proportional to the slope of the phase change, $d\varphi_{A(B)}/d\varepsilon$, it can be extended by increasing the slope. This may be done with the help of a resonance mode introduced by changing the NS interface into a NSNS structure. We denote the widths of first superconductor barrier and next normal conductor as d and L , respectively. The phase $\varphi_A(\varepsilon)$ for plane waves in the NSNS case is shown in Fig. 2 (b): the slope becomes steeper as d increases, eventually approaching an abrupt 2π phase jump at the resonance point.

Now consider a Gaussian wavepacket, beginning with the normally incident case, $\vec{k}_0 = (k_{0x}, 0)$. For the window function $\mathcal{G}(\vec{k})$ in Eq. (9), we take $k_{0x} = \frac{k_F + k_M}{2}$, where $k_M = \sqrt{k_F^2 + \frac{2m}{\hbar^2} \Delta}$, and $\sigma = \frac{k_M - k_F}{n}$, $n = 4$ and 5 for the NS and NSNS interface. The k_x dependence of the window function is given by $g(k_x) = \mathcal{G}(k_x, 0)$, and it corresponds to $g(\varepsilon) = e^{-(\varepsilon - \varepsilon_0)^2 / \sigma_\varepsilon^2}$, $\varepsilon_0 = \Delta/2$ and $\sigma_\varepsilon = \Delta/n$, which are shown as blue line in the upper pannels in 2

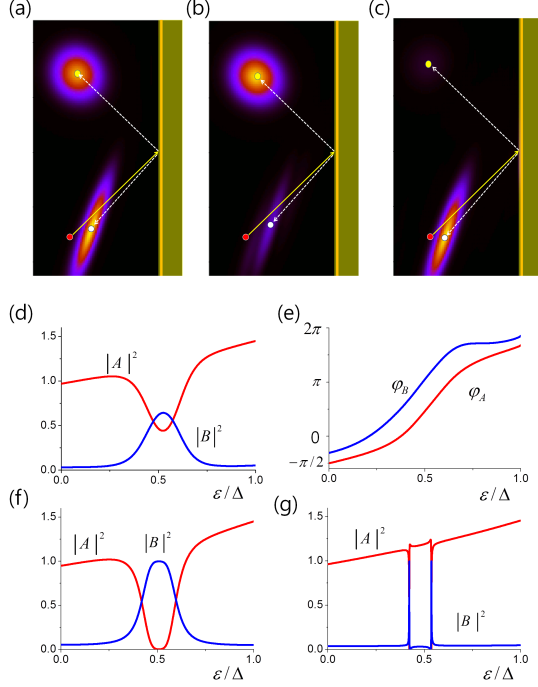


FIG. 4: (color online) Various resonant reflections when $\Delta = 0.2E_F$. (a) $(d, L) = (3, 13)$. (b) $(d, L) = (4.7, 13)$. (c) $(d, L) = (20, 13)$ in the unit of \AA . The red dots denote the initial position and white and yellow dots correspond to the final positions of hole and electron, respectively. Note that the incident-electron velocity is not parallel to the reflected-hole velocity in this large Δ case, because both are parallel to radial lines of Fermi circle as shown in Fig. 1 (a). The scale of the normal conductor shown above is $(0.12\mu\text{m} \times 0.24\mu\text{m})$. (d),(f),(g) $|A|^2$ and $|B|^2$ as a function of ε/Δ for the cases of (a),(b),(c), respectively. (e) The phases, φ_A and φ_B for the $(d, L) = (3, 13)$ case (see supplemental material for wave-packet animations).

(a),(b). The wave-packet movements are shown in the lower pannels. The red line and blue line describe the incident-electron and reflected-hole wave packets, respectively. For the NS interface in Fig. 2 (a), we can see some distance between wave packets of electron at $t = -8$ and hole at $t = 8$, correspondig to the delay length, $l_D = v_F \delta t$ (note $|v_e| \simeq |v_h| \simeq v_F$ in this case, v_e and v_h are electron and hole group velocities). For the resonant reflection in Fig. 2 (b), a longer time delay is expected from the steeper slope of $\varphi_A(\varepsilon)$, and the extended delay length is clearly shown in the lower panel of Fig. 2 (b).

Now consider a finite incidence angle, i.e., $k_{0y} \neq 0$; here one might expect a GH shift for the reflected hole like the l_h in Fig. 1 (b), based on the separability of x and y coordinates like for a diagonal step potential. However, this is not the case. The wave-packet dynamics are illustrated in Fig. 2 (c)-(e). Figure 2 (c) shows the incident wave packet with 45 degree incident angle. The retro-reflected hole packets are shown in Fig. 2 for the NS interface (d) and for the NSNS interface (e), for two

times symmetrically before and after the time of impact on the interface. From the distance l_D between initial and final position of the wave packet it is clear that there is a time delay, but no GH shift at all. This can be understood by the dependence of the energy ε on k_y , i.e., $\varepsilon = \frac{\hbar^2}{2m}(k_x^2 + k_y^2) - E_F$. This gives rise to a time delay δt_y^A in the y -direction too, and this time delay is the same as δt_x^A . Thus we see only time delay without GH shift in Fig. 2 (d),(e). The deformed shape of the hole wave packet comes from the relation between k_x and k_h^N . In other words, the symmetric Gaussian window $\mathcal{G}(k_x, k_y)$ becomes (approximately) an asymmetric Gaussian windows in (k_h^N, k_y) plane, as depicted in Fig. 1 (a).

We now turn to a discussion of the more general case where Δ/E_F is not small. As Δ/E_F increases the nature of the reflected object changes from purely Andreev- to mixed Andreev- and specularly-reflected [16]. Figure 3 shows how the coefficients A , B and the delay time δt change as Δ increases. $|A|^2$ and $|B|^2$ and the phases φ_A and φ_B are shown, as a function of ε , in Fig. 3 (a),(b), where the dashed lines are for $\Delta = 0.2E_F$ case and the solid lines are for $\Delta = 0.8E_F$ case. When $\Delta = 0.2E_F$, the coefficients indicate almost pure Andreev reflection ($|A| = 1$ and $|B| = 0$). At $\Delta = 0.8E_F$, $|B|^2$ becomes appreciable so specular reflection becomes important. Fig. 3 (b) implies that $(d\varphi_{A,B}/d\varepsilon) \sim 1/\Delta$ so that the delay time behaves as $\delta t \sim 1/\Delta$, which is drawn in Fig. 3 (d). In Fig. 3 (c), $|A|^2$, $|B|^2$ measured at $\varepsilon = 0.5\Delta$ are shown as a function of Δ , indicating again the non-negligible specular electron reflection for a large Δ .

It is interesting that the resonant reflection in the large Δ case exhibits a dramatic change of the reflected object depending on the width of the superconductor barrier, d . As an example, the various reflections, when $\Delta = 0.2E_F$, are shown in Fig. 4. Here we take $L = 13\text{\AA}$, which supports a resonance mode around $\varepsilon = 0.5\Delta$ for the 45 degree incident angle. As shown in Fig. 4 (a), both electron and hole are reflected out at $d = 3\text{\AA}$, and then electron-dominant reflection is observed at $d = 4.7\text{\AA}$, contrast to Andreev reflection of the small Δ case. For $d = 20\text{\AA}$, we see the hole-dominant reflection, back to Andreev reflection.

This rather peculiar behavior can be understood as an effect of the resonance mode. Figures 4 (d-g) show variation of $|A|^2$ and $|B|^2$ around the resonant point for the above three different cases. For thin barrier case, $d = 3\text{\AA}$, the resonance mode is quite leaky so that the resonance mode affects on the coefficients within a rather broad range in ε , resulting comparable values of $|A|^2$ and $|B|^2$ at the resonant point (see Fig. 4 (d)). Their delay time has a similar value as expected from the slope of the phase variation in Fig. 4 (e). As increasing the barrier width, the broad range is getting narrower and reach its maximum, $|A|^2 = 0$ and $|B|^2 = 1$ (see Fig. 4 (f)). If the barrier width is getting thicker, the single peak structure starts to split into a double-peak structure, showing $|A|^2 = 0$ and $|B|^2 = 1$ at each peak positions, and the width of peaks is getting narrower as shown in Fig.

4 (g). This double-peak structure of a resonance mode is a characteristic feature of two-component resonance where each component has its own wavelength [22].

In conclusion we have studied wave-packet dynamics at NS interface, and found that the GH effect is amplified by the factor E_F/Δ . Interestingly, the effect appears only as a large time delay, hence “sticky”, without any lateral shift. We also demonstrated that in NSNS interface the GH effect is even further enhanced by a resonance mode and for a large Δ the transition from Andreev to specular electron reflection occurs when the decay rate of the

resonance increases. Although we have focussed on the incident electron case, all intriguing features discussed in this Letter can also be found in the incident hole case. We believe that the time-delay effect can be confirmed by an experimental observation, since direct observation of Andreev-reflected electrons in clean systems (where the motion is practically ballistic) is possible [15].

Acknowledgements G.G. acknowledges support from the Ministry of Education and Science of Serbia (Project III45010); A. L. thanks O. Tieleman for stimulating discussions.

-
- [1] F. Goos and H. Hänchen, Ann. Phys. (Leipzig) **436**, 333 (1947).
 - [2] C. W. J. Beenakker, R. A. Sepkhanov, A. R. Akhmerov, and J. Tworzydło, Phys. Rev. Lett. **102**, 146804 (2009).
 - [3] Manish Sharma and Sankalpa Ghosh, J. Phys.: Condens. Matter **23**, 055501 (2011).
 - [4] W. Löffler, A. Aiello, and J. P. Woerdman, Phys. Rev. Lett. **109**, 213901 (2012).
 - [5] S.-Y. Lee, J.-W. Ryu, T.-Y. Kwon, S. Rim, and C.-M. Kim, Phys. Rev. A **72**, 061801(R) (2005).
 - [6] H. Schomerus and M. Hentschel, Phys. Rev. Lett. **96**, 243903 (2006).
 - [7] J. Unterhinninghofen, J. Wiersig, and M. Hentschel, Phys. Rev. E **78**, 016201 (2008).
 - [8] V.-O. de Haan, J. Plomp, T. M. Rekveldt, W. H. Kraan, and A. A. van Well, Phys. Rev. Lett. **104**, 010401 (2010).
 - [9] J. Hawkes and I. Latimer, *Laser; Theory and Practice* (Prentice-Hall, Englewood Cliffs, NJ, 1995).
 - [10] E. P. Wigner, Phys. Rev. **98** 145 (1955).
 - [11] H. Friedrich and J. Trost, Phys. Rev. Lett. **76**, 4869 (1996); Phys. Rev. A **54** 1136 (1996).
 - [12] A. F. Andreev, Sov. Phys. JETP **19**, 1228 (1964).
 - [13] C. W. J. Beenakker, Phys. Rev. Lett. **97**, 067007 (2006).
 - [14] E. Zapata, F. Sols, Phys. Rev. Lett. **102**, 180405 (2009).
 - [15] P. A. M. Benistant, H. van Kempen and P. Wyder, Phys. Rev. Lett. **51** 817 (1983); M. P. Enrico, S. N. Fisher, A. M. Guenault, G. R. Pickett, and K. Torizuka, Phys. Rev. Lett. **70** 1846 (1993).
 - [16] B. V. Schaeybroeck and A. Lazarides, Phys. Rev. Lett. **98**, 170402 (2007); Phys. Rev. A **79**, 053612 (2009).
 - [17] M. W. Zwiernik, C. H. Schunck, A. Schirotzek, and W. Ketterle, Nature (London) **442**, 54 (2006); Science **311**, 492 (2006).
 - [18] G. B. Partridge, W. Li, R. I. Kamar, Y. A. Liao, and R. G. Hulet, Science **311**, 503 (2006); G.B. Partridge, W. Li, Y.A. Liao, R.G. Hulet, M. Haque, and H.T.C. Stoof, Phys. Rev. Lett. **97**, 190407 (2006).
 - [19] P. G. de Gennes, *Superconductivity of Metals and Alloys*, (Westview Press, Advanced Book Program, 1999).
 - [20] G. E. Blonder, M. Tinkham, T. M. Klapwijk, Phys. Rev. B **25** 4516 (1982).
 - [21] W. L. McMillan, Phys. Rev. **175**, 559 (1968).
 - [22] S.-Y. Lee et al. (unpublished)